Published in final edited form as:
Eur Radiol. 2011 September ; 21(9): 1970–1978. doi:10.1007/s00330-011-2130-6.

Incremental Value of Diffusion Weighted and Dynamic Contrast Enhanced MRI in the Detection of Locally Recurrent Prostate Cancer after Radiation Treatment: Preliminary Results

Oguz Akin,
Memorial Sloan-Kettering Cancer Center, Radiology

David Gultekin,
Memorial Sloan-Kettering Cancer Center, Medical Physics

Hebert Alberto Vargas,
Memorial Sloan-Kettering Cancer Center, Radiology

Junting Zheng,
Memorial Sloan-Kettering Cancer Center, Epidemiology and Biostatistics

Chaya Moskowitz,
Memorial Sloan-Kettering Cancer Center, Epidemiology and Biostatistics

Xin Pei,
Memorial Sloan-Kettering Cancer Center, Radiation Oncology

Dahlia Sperling,
Memorial Sloan-Kettering Cancer Center, Radiation Oncology

Lawrence Schwartz,
Columbia University College of Physicians & Surgeons, Radiology

Hedvig Hricak, and
Memorial Sloan-Kettering Cancer Center, Radiology

Michael Zelefsky
Memorial Sloan-Kettering Cancer Center, Radiation Oncology

Abstract

Objectives—To assess the incremental value of diffusion-weighted and dynamic contrast-enhanced MRI to T2-weighted MRI in detecting locally recurrent prostate cancer after radiotherapy.

Methods—Twenty-four patients (median age, 70 years) with a history of radiotherapy-treated prostate cancer underwent multi-parametric MRI (MP-MRI) and transrectal prostate biopsy. Two readers independently scored the likelihood of cancer on a 1-5 scale, using T2WI alone and then adding DWI and DCE-MRI. Areas under receiver operating characteristic curves (AUCs) were estimated at the patient and prostate-side levels. The ADC from DW-MRI and the K^{trans}, k_{ep}, v_e, AUGC90 and AUGC180 from DCE-MRI were recorded.

Results—Biopsy was positive in 16/24 (67%) and negative in 8/24 (33%) patients. AUCs for readers 1 and 2 increased from 0.64 and 0.53 to 0.95 and 0.86 with MP-MRI, at the patient level,

Corresponding Author: Oguz Akin, MD, akino@mskcc.org, 1275 York Avenue, Memorial Sloan-Kettering Cancer Center, Department of Radiology, New York, NY 10065, Tel: (+1) 212-639-3458, Fax: (+1) 212-794-4010.

and from 0.73 and 0.66 to 0.90 and 0.79 with MP-MRI, at the prostate-side level (p values <0.05). Biopsy-positive and biopsy-negative prostate sides differed significantly in median ADC [1.44 vs. 1.68 ($\times 10^{-3}$ mm^2/s)], median K^{trans} [1.07 vs. 0.34 (1/min)], and k_{ep} [2.06 vs 1.0 ($\times$ 1/min)] (p values <0.05).

Conclusions—MP-MRI was significantly more accurate than T2WI alone in detecting locally recurrent prostate cancer after radiotherapy

Keywords

prostate; MRI; diffusion-weighted MRI; dynamic contrast-enhanced MRI; functional imaging

INTRODUCTION

Approximately 30% to 50% of patients who undergo radiation therapy for prostate cancer experience biochemical recurrence within five years [1,2]. Biochemical recurrence is strictly defined as a rise in serum prostate-specific antigen (PSA) by 2 ng/ml or more above the nadir PSA level (Radiation Therapy Oncology Group - American Society of Radiation Oncology “Phoenix” Consensus 2006) [3]. Although serum PSA level measurement is commonly used to monitor patients, the assessment of prostate cancer recurrence after radiation therapy is a clinical challenge. One problem is that the serum PSA level can fluctuate (bounce) after radiation treatment for reasons other than cancer recurrence [4,5]. Furthermore, the serum PSA level is not reliable for differentiating between local and distant recurrence. Yet this differentiation is crucial for patient counseling, as management options may vary from local salvage therapy to systemic therapy depending on the disease status [6,7].

In this setting, medical imaging plays an important role in differentiating local recurrence from distant metastatic disease. Imaging techniques are useful in detecting distant metastases, such as those in the bone, and in assessing lymph node invasion [8]. Still, precise delineation of the location and extent of recurrent tumor within the prostate after radiation therapy continues to be difficult with all imaging techniques [8, 9]. MRI is sometimes used to assess local recurrence after radiation therapy. However, tissue changes such as glandular atrophy and fibrosis induced by radiation cause a decrease in T2-weighted signal intensity within the prostate and make cancer lesions less conspicuous compared with benign prostatic tissue [8, 10].

Functional MRI techniques such as magnetic resonance spectroscopic imaging (MRSI), diffusion-weighted MRI (DW-MRI), and dynamic contrast-enhanced MRI (DCE-MRI) are garnering increasing interest as a possible means of improving the capabilities of conventional MRI for a range of oncological applications, from cancer detection to the assessment of treatment response. Preliminary studies on the use of functional MRI methods to detect locally recurrent prostate cancer after radiation treatment have yielded promising results [11-15]. However, these studies have evaluated functional MRI techniques individually rather than in combination with each other; furthermore, not all of the studies have included quantitative image analysis, and thus it is difficult to compare their findings [11-15].

Recently, it has been suggested that the best possible characterization of prostate cancer would most likely be achieved by a multi-parametric approach supplementing conventional MRI with more than one functional technique [16]. Yet many uncertainties linger regarding how best to analyze, interpret, and integrate the large amount of imaging data generated by this kind of approach [16]. Thus, the purpose of our study was to assess the incremental value of quantitative and qualitative data from DW-MRI and DCE-MRI to conventional

T2WI in the detection of locally recurrent prostate cancer after radiation treatment, using transrectal ultrasound-guided biopsy as the reference standard.

MATERIALS AND METHODS

The institutional review board approved our retrospective study and waived the informed consent requirement. Our study was compliant with the Health Insurance Portability and Accountability Act.

Eligibility Criteria and Patient Characteristics

At our institution, patients in whom recurrence is suspected clinically (biochemical failure as defined by the "Phoenix" consensus [3], or consecutively rising PSA but still insufficient to fulfill the "Phoenix" criteria) are generally offered an endorectal-coil prostate MRI and a TRUS-guided prostate biopsy as part of their assessment. Between April 2008 and September 2009, 24 patients (median age, 70 years; range, 48-82 years) treated for clinically localized prostate cancer were identified in follow-up radiotherapy clinics with a rising PSA profile after treatment (minimum of 2 consecutive rising values) and underwent multi-parametric MRI for evaluation of the extent of their disease followed by a TRUS-guided prostate biopsy(12-16 cores). The biopsies were interpreted by a team of dedicated genitourinary oncology pathologists at our institution, a tertiary academic cancer center. The patients' characteristics are tabulated (Table 1). The median baseline serum PSA level (before radiation therapy) was 6.8 ng/mL (range, 1.1 - 53 ng/mL). The Gleason scores at initial diagnosis were 3+3 in 8 patients (33%), 3+4 in 8 patients (33%), 4+3 in 5 patients (21%) and 4+4 in 3 patients (13%). Eighteen patients received external beam radiation therapy (median dose 8640 cGy), five patients received permanent interstitial implantation with I-125 (prescription dose 144 Gy), and one patient was treated with a combination of brachytherapy (110 Gy I-125) followed by 50.4 Gy intensity-modulated radiation therapy. Ten patients (42%) received neo-adjuvant hormone therapy. The patients' median post-treatment PSA level at the time of the MRI performed for this study was 1.63 ng/mL (range, 0.43 - 6.3 ng/mL). The median time period from radiation therapy to MRI was 43.6 months (range, 17 - 113.7 months). The median time between MRI and transrectal biopsy was 31 days (range, 7-223 days). The clinical and biochemical profile of all patients remained stable between the time the MRI was performed and the transrectal biopsy.

MRI Acquisition, Analysis and Interpretation

Magnetic resonance imaging studies were performed using a 1.5-Tesla MRI in 20 patients and a 3-Tesla MRI in 4 patients (GE Medical Systems, Milwaukee, WI, USA). A pelvic phased-array coil and a balloon-covered expandable endorectal coil (Medrad, Warrendale, PA, USA) were used for imaging. The anatomical images were obtained using transverse, coronal, and sagittal T2-weighted fast spin-echo images of the prostate and seminal vesicles. DW-MRI and DCE-MRI images were obtained in the transverse plane with orientation and location identical to those prescribed for the transverse T2-weighted anatomical images. DW-MRI was acquired using a single-shot spin-echo echo-planar imaging sequence with diffusion encoding *b*-values of 0, 400 and 700 s/mm^2 along three orthogonal axes. DCE-MRI was acquired using a 3D T1-weighted spoiled gradient echo sequence with a temporal resolution of about 7-8 seconds covering the entire prostate over 4–5 minutes following intravenous injection of 0.1 mmol/kg body weight gadolinium-DTPA (Magnevist, Berlex Labs, Montville, NJ, USA) at a rate of 2 mL/s using an automatic injector (Medrad, Warrendale, PA, USA).

Magnetic resonance imaging studies were archived in a Picture Archiving and Communication System (Centricity; GE Medical Systems, Milwaukee, WI, USA). DW-MRI

and DCE-MRI data were analyzed using Advanced Workstation and KinMod research software (GE Medical Systems), IDL (ITT, Boulder, CO, USA) and Matlab (Mathworks, Natick, MA, USA). Multi-parametric MRI datasets were converted into color-coded images on a pixel-by-pixel basis reflecting the apparent diffusion coefficient (ADC) from DW-MRI; and the rate of contrast agent transfer from vascular space to extravascular and extracellular space (K^{trans}), the rate constant from extravascular and extracellular space to vascular space (k_{ep}), the fractional extravascular and extracellular volume (v_e), and the initial area under the gadolinium concentration-time curve (AUGC) from DCE-MRI [17, 18].

Two radiologists independently interpreted MRI studies. Reader 1 was a genitourinary radiologist with six years of experience in interpreting prostate MRI. Reader 2 was a final year radiology trainee undergoing dedicated research experience in genitourinary imaging who had received dedicated instruction and reviewed approximately 200 prostate MRI prior to this study. Although the readers were aware that the patients had received radiation treatment for prostate cancer, they were blinded to clinical and laboratory findings (including PSA values) as well as histological and imaging findings.

Qualitative Assessment—The readers evaluated six regions of the prostate: the right and left base, mid-gland and apex. For all regions (i.e., sextants), the readers independently assigned scores for the likelihood of cancer on a 1-5 index scale (1: definitely absent; 2: probably absent; 3: indeterminate; 4: probably present; 5: definitely present). First they assigned scores based on the interpretation of T2-weighted images alone. Then, they evaluated each sextant using multi-parametric MR imaging (i.e., a combination of T2-weighted, DW-MR and DCE-MR images) and assigned a new set of scores. For the purposes of image interpretation, recurrent tumor was defined as a focal or nodular area that displayed (i) low signal intensity on T2-weighted images; (ii) restricted diffusion on diffusion-weighted images; and (iii) avid enhancement with wash-out on DCE-MRI (Fig. 1).

Quantitative Assessment—For quantitative analysis of DW-MRI and DCE-MRI datasets, a region of interest (ROI) was placed in each sextant of the prostate to cover the focal area most suspicious for prostate cancer within that sextant based on the readers' qualitative assessment (if no area was considered suspicious, then the ROI was placed in an area of normal tissue). Within each ROI, the mean, range, and standard deviation of the following six quantitative parameters were recorded: ADC from diffusion-weighted MRI, and K^{trans}, k_{ep}, v_e, AUGC90 (AUGC over 90 seconds) and AUGC180 (AUGC over 180 seconds) from DCE-MRI.

Statistical Methods

Reader performance in qualitative assessment of MRI studies was analyzed at both the patient and the prostate-side level. At the patient level, we used the readers' maximum qualitative scores for the likelihood of recurrent tumor of the sextants, and at the prostate-side level, we used the maximum qualitative score of the corresponding regions. Receiver operating characteristic (ROC) curves and the empirical area under the curve (AUC) together with 95% confidence intervals (CIs) were estimated separately for the patient and prostate-side levels with a non-parametric method taking into account the clustered data for the side-level analysis [19, 20].

The quantitative MRI parameters (ADC, K^{trans}, k_{ep}, v_e, AUGC90 and AUGC180) were analyzed at the prostate-side level by assigning the highest ROI value for each parameter on that side of the prostate. The median and range values for each quantitative MRI parameter were summarized as continuous variables. Generalized estimating equation analysis was

used to test the association between each parameter with the biopsy result adjusting for the correlation between multiple observations made within a patient.

For patient characteristics, the Wilcoxon rank-sum test was used to compare the continuous variables; Fisher's exact test was used to examine the association between the categorical variables. P values < 0.05 were considered statistically significant and no adjustment of p values was performed considering the hypothesis-generating nature of the study. To evaluate the agreement between the two readers, weighted Kappa coefficients were calculated. All statistical analyses were performed with a software package (SAS 9.2; SAS Institute Inc., Cary, NC, USA).

RESULTS

Patient Characteristics

In our study group of 24 men, TRUS-guided biopsy was positive for locally recurrent prostate cancer in 16 (67%) and negative in 8 (33%). The Gleason scores of the 16 patients with positive biopsies were: Gleason 3+4: 5 patients; Gleason 4+3: 5 patients; Gleason 4+4: 4 patients and Gleason 4+5: 1 patient. Compared to the Gleason score at initial diagnosis, the Gleason score at the time of recurrence was higher in 7/16 patients (44%) and stable in 8/16 patients (50%). In 1/16 patients (6%), the biopsy Gleason score was not provided. TRUS-guided biopsy was positive in 22 of 48 prostate sides (46%) and negative in 26 (54%). Recurrence was unilateral in 10/16 patients (63%) and bilateral in 6/16 patients (37%). The clinical characteristics of the patients with and without positive biopsy findings did not differ significantly (Table 1).

Biochemical Failure Status—Based on the Phoenix Consensus 2006 definition of biochemical failure (a rise in PSA of > 2 ng/ml above the nadir level) [3], seven patients (29%) had biochemical failure and seventeen patients (71%) did not. Twelve (71%) of the 17 patients who did not meet the criteria for biochemical failure had recurrent tumor in the prostate confirmed by TRUS-guided biopsy. In this highly-selected small cohort of patients, we did not observe any statistically significant association between the biochemical failure status and the TRUS-guided biopsy result (Fisher's exact test p=0.647).

MRI Results

Qualitative Assessment—Our results showed that the addition of multi-parametric images from DW-MRI and DCE-MRI to T2-weighted images significantly improved both readers' performance in detecting locally recurrent prostate cancer after radiation treatment. At the patient level, the AUC for reader 1 increased from 0.64 (95% CI: 0.43-0.85) with T2-weighted MRI alone to 0.95 (95% CI: 0.87-1.00) with multi-parametric MRI (p=0.002), and the AUC for reader 2 increased from 0.53 (95% CI: 0.31-0.75) with T2-weighted MRI alone to 0.86 (95% CI: 0.73-0.99) with multi-parametric MRI (p=0.012) (Fig. 2a). At the prostate-side level, the AUC for reader 1 increased from 0.73 (95% CI: 0.57-0.88) with T2-weighted MRI alone to 0.90 (95% CI: 0.74-1.00) with multi-parametric MRI (p<0.001), and the AUC for reader 2 increased from 0.66 (95% CI: 0.54-0.78) with T2-weighted MRI alone to 0.79 (95% CI: 0.65-0.93) with multi-parametric MRI (p=0.003) (Fig. 2b). In addition, inter-reader agreement was higher for the interpretation of multi-parametric MRI than for the interpretation of T2-weighted MRI alone, with the weighted Kappa statistic increasing from 0.38 to 0.79 at the patient level and 0.32 to 0.61 at the prostate-side level.

We dichotomized the five-point qualitative suspicion index to assess the sensitivity and specificity for each reader at both the patient and prostate-side levels. We explored two cutoff points. Cutoff point 1was defined as follows: 1-2, no tumor; 3-5, tumor; cutoff point 2

was defined thus: 1-3, no tumor; 4-5. Table 2 summarizes the readers' sensitivity and the specificity values at these two cutoff points (Table 2).

Quantitative Assessment—Table 3 and Fig. 3 summarize the quantitative MRI parameters (ADC, K^{trans}, k_{ep}, v_e, AUGC90, and AUGC180) which were analyzed at the prostate-side level by assigning the highest ROI value for each parameter to the positive or negative group according to the biopsy result on that side of the prostate. We found a significant difference in the median ADC values obtained from the biopsy-positive and the biopsy-negative prostate sides (p=0.012) (Table 3, Fig. 3). There were also significant differences in the median K^{trans} values (p=0.010) and the median k_{ep} values (p=0.008) obtained from the biopsy-positive and the biopsy-negative prostate sides (Table 3, Fig. 3). The median v_e, AUGC90, and AUGC180 did not differ significantly between the biopsy-positive and the biopsy-negative prostate sides (Table 3, Fig. 3).

DISCUSSION

In our patient population, the functional multi-parametric MRI techniques performed remarkably well in detecting recurrent prostate cancer after definitive radiation treatment. When DW- and DCE-MR images were added to T2-weighted MRI, accuracy in the detection of local recurrence at the patient and prostate-side levels increased significantly for both an experienced reader and an inexperienced reader. Furthermore, the addition of MP-MRI resulted in greater inter-reader agreement in qualitative image interpretation at both the patient and the prostate-side levels.

Our results also suggest that quantitative analysis of MP-MRI could play an important role in identifying locally recurrent prostate cancer. In DW-MRI, the median ADC measurement obtained from the biopsy-positive prostate sides was significantly lower than that obtained from the biopsy-negative sides. In addition, quantitative pharmacokinetic analysis of DCE-MRI data showed significant differences in the median values of the transfer rate constants K^{trans} and k_{ep} obtained from the biopsy-positive and the biopsy-negative prostate sides.

Sala et al. studied the accuracy of conventional (T2-weighted) MRI to evaluate the localization and staging of recurrent cancer in the prostate after radiation therapy in 45 patients using pathological assessment of the salvage prostatectomy specimens as the reference standard [10]. In their study, the areas under the receiver operating characteristic curves (AUCs) for two radiologists were 0.61 and 0.75 for recurrent tumor localization within the prostate. A number of other small studies have explored the potential of functional techniques to improve the MR imaging assessment of locally recurrent prostate cancer after radiation treatment and have yielded promising results. In a study of 21 patients with post-radiotherapy biochemical failure, which used subsequent TRUS-guided biopsy as the reference standard, Coakley et al. found that MRSI was substantially more accurate than conventional MRI in the detection of local recurrence in the prostate (AUCs were 0.81 for MRSI and 0.49 and 0.51 (two readers) for MRI) [11]. Pucar et al. performed a similar study in 9 patients with post-radiotherapy biochemical recurrence, using step-section pathological maps of salvage prostatectomy specimens as the reference standard. They found that MRI and MRSI had sensitivities of 68% and 77%, respectively, in the detection of local recurrence, while biopsy and digital rectal examination had sensitivities of just 48% and 16%, respectively [12]. They also observed that MRSI could falsely identify metabolically altered benign gland as cancer and had specificity lower than that of MRI, biopsy or digital rectal examination (78% vs. 96%, 95% and 96%, respectively) [12]. In a study of 36 patients with post-radiotherapy biochemical failure that used biopsy results as the reference standard, Kim et al. found that at 3 Tesla, the combination of conventional MRI and DW-MRI was significantly more accurate than conventional MRI alone in predicting locally recurrent

prostate cancer, increasing the AUC from 0.61 to 0.88 ($p < 0.01$) [13]. However, in that study, an endorectal coil was not used to increase the signal-to-noise ratio during imaging [13].

Rouvière et al. compared conventional MRI and DCE-MRI in the detection of post-radiotherapy recurrence in 22 patients, using biopsy results as the reference standard [14]; the three readers achieved higher sensitivities with DCE-MRI than they achieved with conventional MRI (0.70-0.74 versus 0.26-0.44), while the specificities they achieved with the two techniques were similar (0.73-0.85 versus 0.64-0.86) [14]. In addition, inter-observer agreement was greater with DCE-MRI (kappa: 0.63-0.70) than with conventional MRI (kappa: 0.18- 0.39) [14]. However, DCE-MR data could not be analyzed quantitatively because a suboptimal DCE-MRI technique was used, with a low temporal resolution (30 seconds) and images were acquired at only three time points after contrast medium injection [14]. Furthermore, an endorectal coil was not used [14]. In a similar study of 33 patients with post-radiotherapy biochemical recurrence that used biopsy results as the reference standard for tumor detection, a single reader achieved higher sensitivity with DCE-MRI than with conventional MRI (0.72 versus 0.38) but again a similar specificity (0.85 versus 0.80) [15]. The investigators used a low temporal resolution (95 seconds) and image acquisition at seven time points after contrast medium injection, without an endorectal coil [15]. In interpreting DCE-MRI, they defined a region as suspicious for cancer if it showed enhancement in the first post-contrast phase (48 seconds after injection) that was greater than the mean signal intensity of the prostate in the last phase (618 seconds after injection) [15]. Although the DCE-MRI analysis method was easy to carry out, it did not include quantitative analysis of the pharmacokinetic DCE-MRI parameters [15].

Our results are in agreement with those of the above-mentioned studies and support the conclusion that adding MP-MRI techniques to conventional MRI can significantly improve both accuracy and inter-reader agreement in the detection of local prostate cancer recurrence after radiotherapy [11-15]. While we avoided some of the limitations of the previous studies, our study did have limitations, including its retrospective design and small sample size. Also, approximately 2/3 of patients had intermediate or high risk prostate cancer at initial diagnosis (clinical stage >T2a, Gleason score >6 or PSA >10 ng/mL). Although this is probably expected in a group of patients with suspected recurrence following treatment, it is a potential cause of selection bias. Furthermore, the reference standard we used was a TRUS-guided biopsy and not a surgical pathology specimen. Biopsy is a limited method for localizing prostate cancer, particularly in the apical regions, where its sensitivity for detecting prostate cancer is similar to MRI itself [21]. In addition to false negative diagnosis due to sampling errors, post radiotherapy prostate biopsies are difficult to interpret histopathologically, as the presence of malignant cells on biopsy specimens may not represent biologically active tumors, especially in the first 1-2 years after treatment [22-24]. Due to the known limitations involved in co-localizing TRUS-guided biopsy and MRI, we performed our qualitative and quantitative analyses at the patient and prostate-side levels but not at the lesion level. The impact of including patients treated with external beam radiation therapy and brachytherapy, and had MRI performed at 1.5T and 3T on our qualitative and quantitative assessments is unknown, and has not been accounted for, although the effects of higher magnetic field strength on diagnostic accuracy of MRI in prostate cancer has not been clearly established [24]. Furthermore, our estimated measures of accuracy may suffer from verification bias because patients who had MP-MRI but did not undergo transrectal prostate biopsy were excluded.

Accurate identification of the presence and site of prostate cancer recurrence after radiotherapy is of paramount importance for appropriate treatment selection and planning. Patients with local recurrence are potential candidates for local salvage therapy [25],

whereas distant disease is treated with androgen deprivation and/or chemotherapy. Furthermore, identifying recurrence in a timely manner is crucial. A recent study of 2380 patients who underwent primary surgical or radiation treatment for prostate cancer showed that, particularly among patients with high-risk primary disease, surgical treatment was associated with a lower risk of metastatic progression and prostate cancer-specific death than external beam radiation therapy [26]. The authors postulated that the difference in outcome could have been due to differences in the frequency and timing of salvage therapy, as the median time from primary to salvage therapy was 13 months in the surgical group and 69 months in the radiation treatment group [26]. The difficulty of diagnosing locally recurrent prostate cancer after radiation treatment at an early stage is one of the main reasons why local salvage therapy has been under-utilized [7]. We found that multi-parametric MRI performed remarkably well in detecting recurrent cancer in this group. In doing so, MRI has the potential to contribute to the clinical management in this patient population by (i) eliminating unnecessary biopsies, for example in patients with definite MRI evidence of local recurrence, thus avoiding the small risk of potential complications; (ii) guiding "targeted" biopsies, for example in patients with high clinical suspicion for recurrence but negative TRUS-guided biopsies; and (iii) identifying patients who could be candidates for "focal" salvage therapies, such as cryotherapy, high-intensity focused ultrasound and laser ablation.

Acknowledgments

We are grateful to Ms Ada Muellner for her editorial assistance.

References

1. Kuban DA, Thames HD, Levy LB, Horwitz EM, Kupelian PA, Martinez AA, Michalski JM, Pisansky TM, Sandler HM, Shipley WU, Zelefsky MJ, Zietman AL. Long-term multi-institutional analysis of stage T1-T2 prostate cancer treated with radiotherapy in the PSA era. Int J Radiat Oncol Biol Phys. 2003; 57:915–928. [PubMed: 14575822]
2. Zietman AL, DeSilvio ML, Slater JD, Rossi CJ Jr, Miller DW, Adams JA, Shipley WU. Comparison of conventional-dose vs high-dose conformal radiation therapy in clinically localized adenocarcinoma of the prostate: a randomized controlled trial. JAMA. 2005; 294:1233–1239. [PubMed: 16160131]
3. Roach M 3rd, Hanks G, Thames H Jr, Schellhammer P, Shipley WU, Sokol GH, Sandler H. Defining biochemical failure following radiotherapy with or without hormonal therapy in men with clinically localized prostate cancer: recommendations of the RTOG-ASTRO Phoenix Consensus Conference. Int J Radiat Oncol Biol Phys. 2006; 65:965–74. [PubMed: 16798415]
4. Denham JW, Kumar M, Gleeson PS, Lamb DS, Joseph D, Atkinson C, Matthews J, Tai KH, Spry NA, Christie D, Turner S, Greer PB, D'Este C, Steigler A. Recognizing false biochemical failure calls after radiation with or without neo-adjuvant androgen deprivation for prostate cancer. Int J Radiat Oncol Biol Phys. 2009; 74:404–11. [PubMed: 19176272]
5. Pickles T. British Columbia Cancer Agency Prostate Cohort Outcomes Initiative. Prostate-specific antigen (PSA) bounce and other fluctuations: which biochemical relapse definition is least prone to PSA false calls? An analysis of 2030 men treated for prostate cancer with external beam or brachytherapy with or without adjuvant androgen deprivation therapy. Int J Radiat Oncol Biol Phys. 2006; 64:1355–9. [PubMed: 16406391]
6. Boccon-Gibod L, Djavan WB, Hammerer P, Hoeltl W, Kattan MW, Prayer-Galetti T, Teillac P, Tunn UW. Management of prostate-specific antigen relapse in prostate cancer: a European Consensus. Int J Clin Pract. 2004; 58:382–90. [PubMed: 15161124]
7. Stephenson AJ, Scardino PT, Bianco FJ Jr, Eastham JA. Salvage therapy for locally recurrent prostate cancer after external beam radiotherapy. Curr Treat Options Oncol. 2004; 5:357–65. [PubMed: 15341674]

8. Akin O, Hricak H. Imaging of prostate cancer. Radiol Clin North Am. 2007; 45:207–22. [PubMed: 17157630]
9. Fuchsjäger M, Akin O, Shukla-Dave A, Pucar D, Hricak H. The role of MRI and MRSI in diagnosis, treatment selection, and post-treatment follow-up for prostate cancer. Clin Adv Hematol Oncol. 2009; 7:193–202. [PubMed: 19398944]
10. Sala E, Eberhardt SC, Akin O, Moskowitz CS, Onyebuchi CN, Kuroiwa K, Ishill N, Zelefsky MJ, Eastham JA, Hricak H. Endorectal MR imaging before salvage prostatectomy: tumor localization and staging. Radiology. 2006; 238:176–83. [PubMed: 16373766]
11. Coakley FV, Teh HS, Qayyum A, Swanson MG, Lu Y, Roach M 3rd, Pickett B, Shinohara K, Vigneron DB, Kurhanewicz J. Endorectal MR imaging and MR spectroscopic imaging for locally recurrent prostate cancer after external beam radiation therapy: preliminary experience. Radiology. 2004; 233:441–8. [PubMed: 15375223]
12. Pucar D, Shukla-Dave A, Hricak H, Moskowitz CS, Kuroiwa K, Olgac S, Ebora LE, Scardino PT, Koutcher JA, Zakian KL. Prostate cancer: correlation of MR imaging and MR spectroscopy with pathologic findings after radiation therapy-initial experience. Radiology. 2005; 236:545–53. [PubMed: 15972335]
13. Kim CK, Park BK, Lee HM. Prediction of locally recurrent prostate cancer after radiation therapy: incremental value of 3T diffusion-weighted MRI. J Magn Reson Imaging. 2009; 29:391–7. [PubMed: 19161194]
14. Rouvière O, Valette O, Grivolat S, Colin-Pangaud C, Bouvier R, Chapelon JY, Gelet A, Lyonnet D. Recurrent prostate cancer after external beam radiotherapy: value of contrast-enhanced dynamic MRI in localizing intraprostatic tumor--correlation with biopsy findings. Urology. 2004; 63:922–7. [PubMed: 15134982]
15. Haider MA, Chung P, Sweet J, Toi A, Jhaveri K, Ménard C, Warde P, Trachtenberg J, Lockwood G, Milosevic M. Dynamic contrast-enhanced magnetic resonance imaging for localization of recurrent prostate cancer after external beam radiotherapy. Int J Radiat Oncol Biol Phys. 2008; 70:425–30. [PubMed: 17881141]
16. Kurhanewicz J, Vigneron D, Carroll P, Coakley F. Multiparametric magnetic resonance imaging in prostate cancer: present and future. Curr Opin Urol. 2008; 18:71–7. [PubMed: 18090494]
17. Padhani AR, Liu G, Koh DM, Chenevert TL, Thoeny HC, Takahara T, Dzik-Jurasz A, Ross BD, Van Cauteren M, Collins D, Hammoud DA, Rustin GJ, Taouli B, Choyke PL. Diffusion-weighted magnetic resonance imaging as a cancer biomarker: consensus and recommendations. Neoplasia. 2009; 11:102–25. [PubMed: 19186405]
18. Tofts PS, Brix G, Buckley DL, Evelhoch JL, Henderson E, Knopp MV, Larsson HB, Lee TY, Mayr NA, Parker GJ, Port RE, Taylor J, Weisskoff RM. Estimating kinetic parameters from dynamic contrast-enhanced T(1)-weighted MRI of a diffusible tracer: standardized quantities and symbols. J Magn Reson Imaging. 1999; 10:223–32. [PubMed: 10508281]
19. DeLong ER, DeLong DM, Clarke-Pearson DL. Comparing the areas under two or more correlated receiver operating characteristic curves: a nonparametric approach. Biometrics. 1988; 44:837–45. [PubMed: 3203132]
20. Obuchowski NA. Nonparametric analysis of clustered ROC curve data. Biometrics. 1997; 53:567–78. [PubMed: 9192452]
21. Wefer AE, Hricak H, Vigneron DB, et al. Sextant localization of prostate cancer: comparison of sextant biopsy, magnetic resonance imaging and magnetic resonance spectroscopic imaging with step section histology. The Journal of Urology. 2000; 164:400–404. [PubMed: 10893595]
22. Cox JD, Gallagher MJ, Hammond EH, Kaplan RS, Schellhammer PF. Consensus statements on radiation therapy of prostate cancer: guidelines for prostate re-biopsy after radiation and for radiation therapy with rising prostate-specific antigen levels after radical prostatectomy. American Society for Therapeutic Radiology and Oncology Consensus Panel. J Clin Oncol. 1999; 17:1155. [PubMed: 10561174]
23. Crook J, Malone S, Perry G, Bahadur Y, Robertson S, Abdolell M. Postradiotherapy prostate biopsies: what do they really mean? Results for 498 patients. Int J Radiat Oncol Biol Phys. 2000; 48:355–367. [PubMed: 10974448]

24. Crook JM, Perry GA, Robertson S, Esche BA. Routine prostate biopsies following radiotherapy for prostate cancer: results for 226 patients. Urology. 1995; 45:624–631. discussion 631-622. [PubMed: 7716843]

25. Park B, Kim B, Kim C, Lee H, Kwon G. Comparison of phased-array 3.0-T and endorectal 1.5-T magnetic resonance imaging in the evaluation of local staging accuracy for prostate cancer. Journal of computer assisted tomography. 2007; 31:534–538. [PubMed: 17882027]

26. Kimura M, Mouraviev V, Tsivian M, Mayes JM, Satoh T, Polascik TJ. Current salvage methods for recurrent prostate cancer after failure of primary radiotherapy. BJU Int. 2010; 105:191–201. [PubMed: 19583717]

27. Zelefsky MJ, Eastham JA, Cronin AM, Fuks Z, Zhang Z, Yamada Y, Vickers A, Scardino PT. Metastasis after radical prostatectomy or external beam radiotherapy for patients with clinically localized prostate cancer: a comparison of clinical cohorts adjusted for case mix. J Clin Oncol. 2010; 28:1508–13. [PubMed: 20159826]

Abbreviations

ADC	apparent diffusion coefficient
MP-MRI	multi-parametric MRI
DW-MRI	diffusion-weighted MRI
DCE-MRI	dynamic contrast-enhanced MRI
T2WI	T2-weighted MRI
AUC	areas under receiver operating characteristic curves
PSA	prostate-specific antigen
MRSI	magnetic resonance spectroscopic imaging
TRUS	transrectal ultrasound
K^{trans}	rate of contrast agent transfer from vascular space to extravascular and extracellular space
k_{ep}	rate constant from extravascular and extracellular space to vascular space
v_e	fractional extravascular and extracellular volume
AUCG	initial area under the gadolinium concentration-time curve

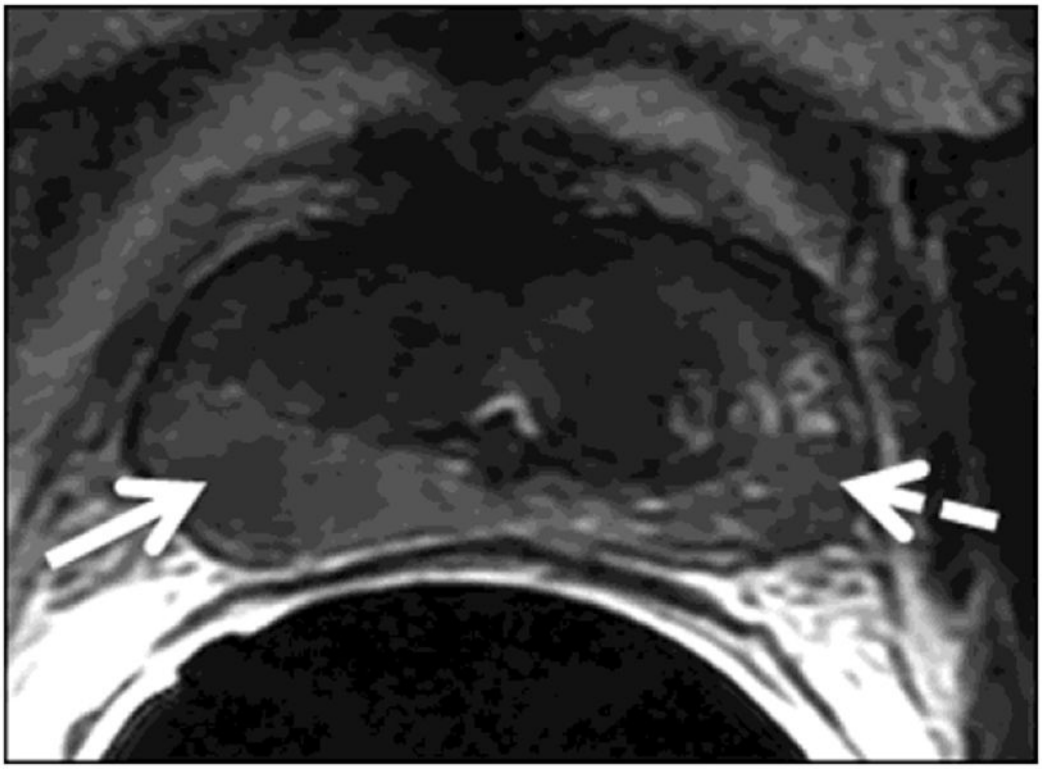

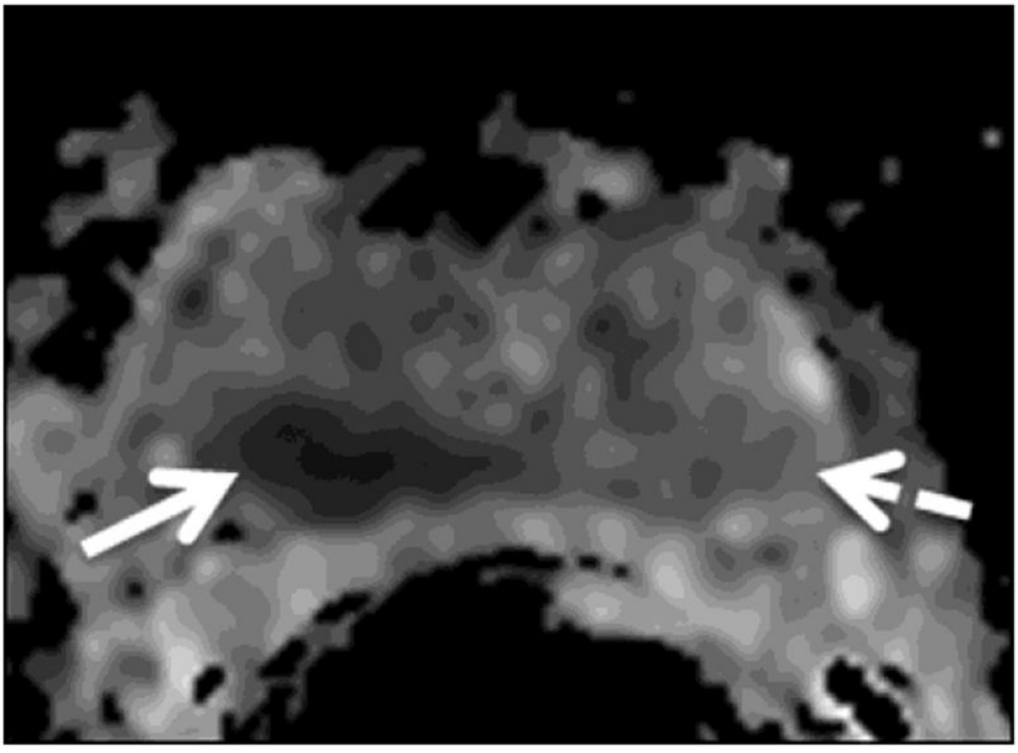

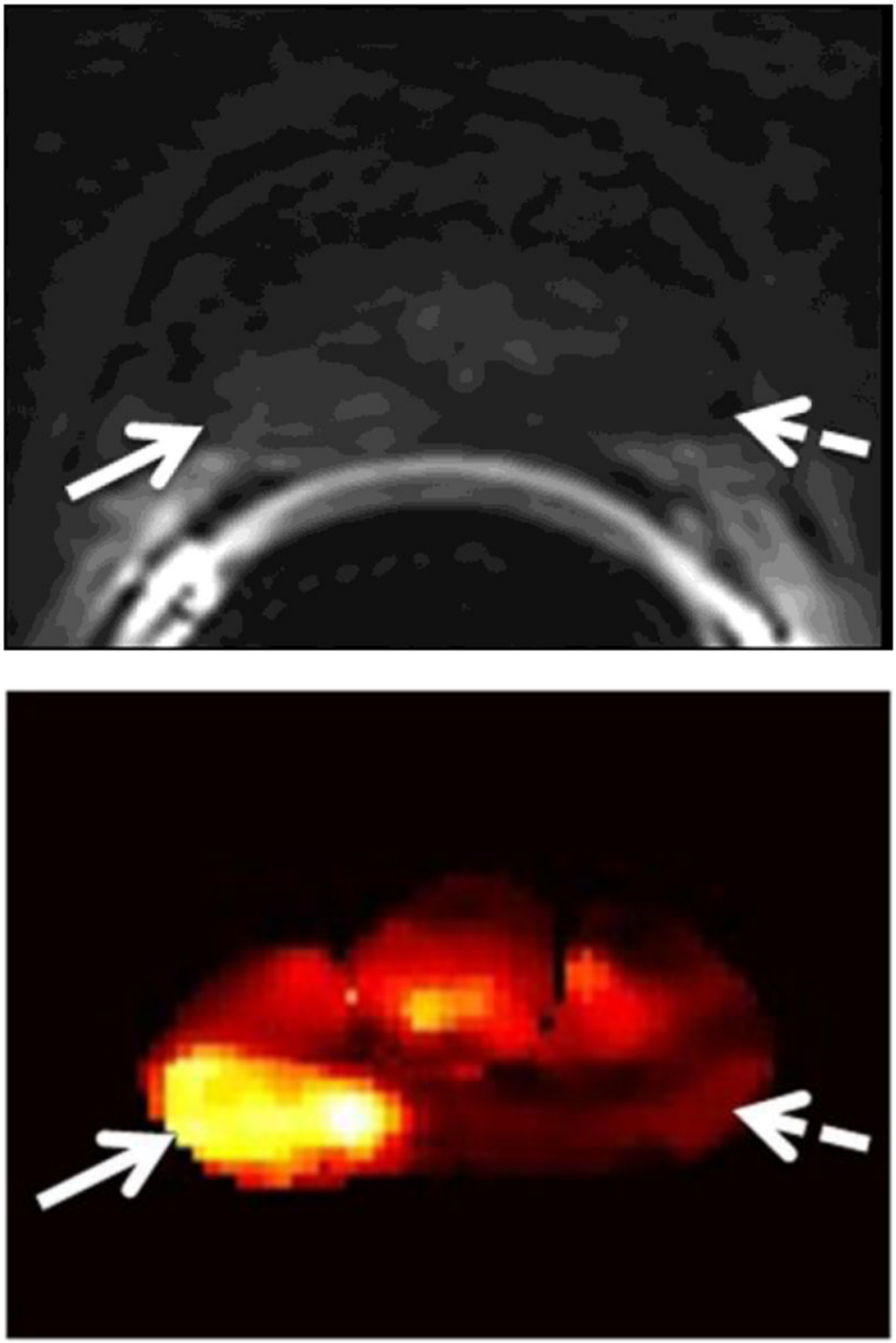

Figure 1.
A 75-year-old man with recurrent Gleason 4+3 tumor (arrows) after radiotherapy. An ill-defined lesion is noted in the right peripheral zone of the prostate on the T2-weighted image

(1a), the tumor becomes more conspicuous on the ADC map (1b), dynamic contrast-enhanced image (1c) and K^{trans} map (1d). Note that there is an ill-defined nodular area (dashed arrow) that could mimic tumor on the contralateral aspect of the prostate on the T2-weighted image (1a); however, ADC map (1b), dynamic contrast-enhanced image (1c) and K^{trans} map (1d) rule out tumor on the left side (dashed arrows).

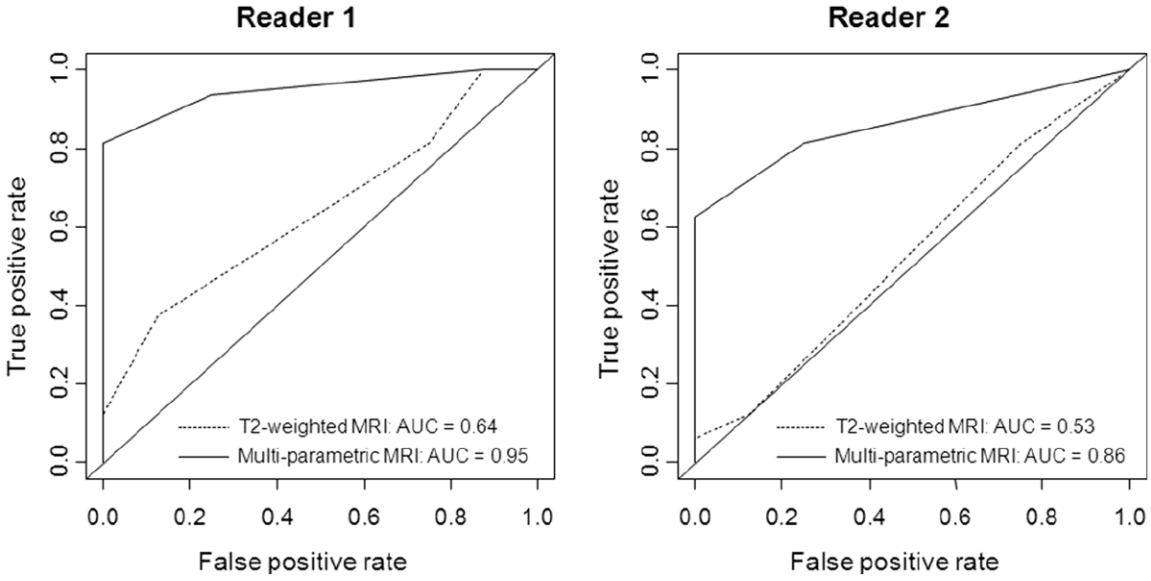

Figure 2.

Graphs show ROC curves and AUCs for each reader as a measure of accuracy for qualitative assessment in detecting locally recurrent prostate cancer after radiation treatment at both the patient level (2a) and the prostate-side level (2b). (Note: reader 1 was an experienced radiologist, whereas reader 2 was less experienced).

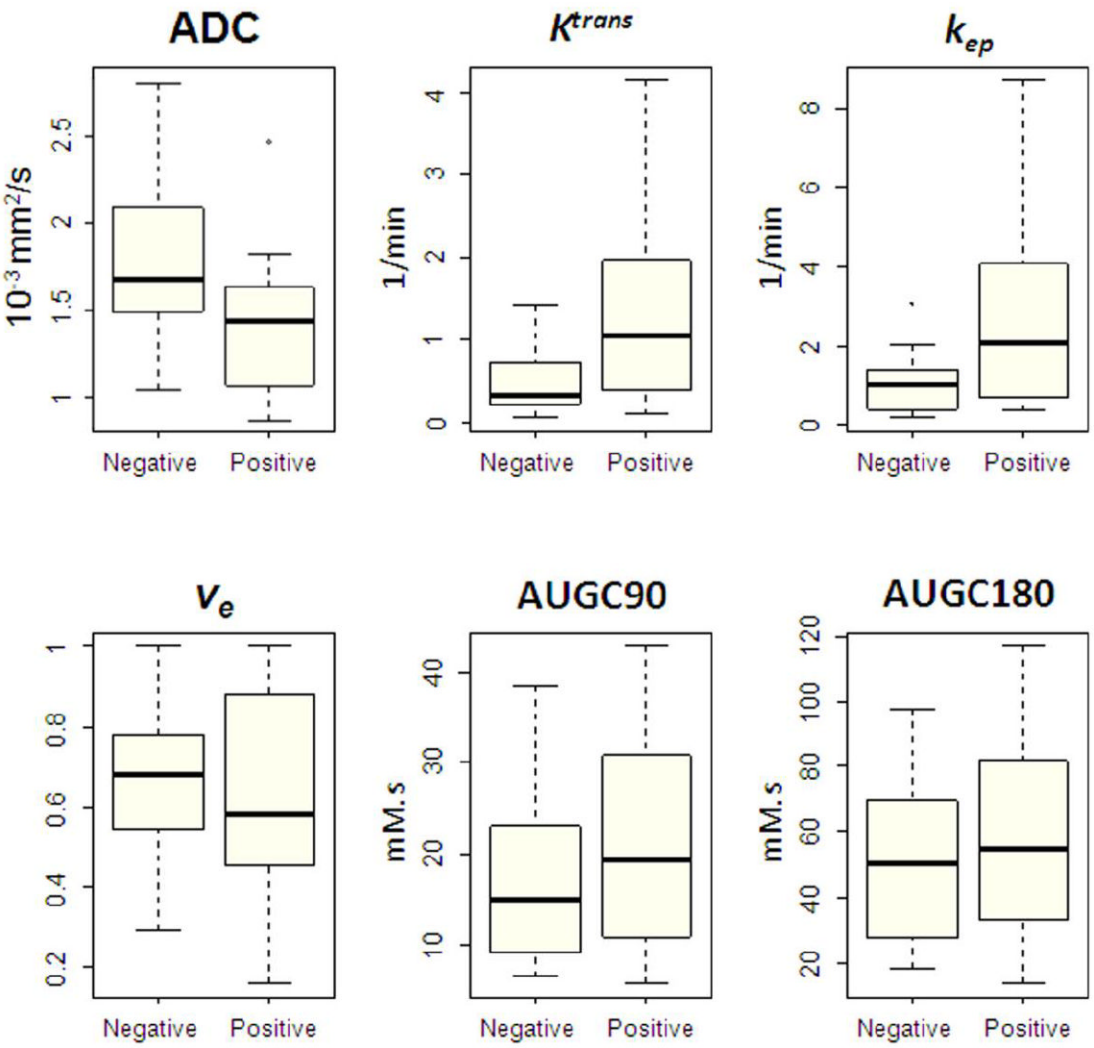

Figure 3.

Box-and-whisker plots illustrate quantitative MRI parameters for biopsy-negative and biopsy-positive prostate sides. *(Note: The boxes represent the values from the lower to the upper quartile; the horizontal line inside each box indicates the median; the horizontal lines outside each box indicate the minimum and maximum values; and the dots indicate outlying values).*

Table 1

Patient Characteristics

	All Patients (n=24)	Patients with Positive Transrectal Biopsy (n=16)	Patients with Negative Transrectal Biopsy (n=8)	p Value
Age[1] (years), median (range)	70.5 (48 - 82)	74.5 (48 - 82)	68.5 (57 - 71)	0.062
Initial PSA (ng/mL), median (range)	6.80 (1.10 - 53.00)	7.03 (1.10 - 53.00)	6.70 (1.75 - 12.00)	0.587
Follow-up PSA[2] (ng/mL), median (range)	1.63 (0.43 - 6.30)	1.47 (0.43 - 6.30)	3.03 (0.44 - 5.50)	0.132
Time since radiation treatment (months), median (range)	43.6 (17.0 - 113.7)	49.3 (17.0 - 92.6)	42.8 (17.4 - 113.7)	1.000
Initial clinical stage, n[3] (%)				
1c	12 (52%)	5 (33%)	7 (88%)	0.075
2a	3 (13%)	3 (20%)	0	
2b	1 (4%)	1 (7%)	0	
2c	3 (13%)	3 (20%)	0	
3a	3 (13%)	3 (20%)	0	
3b	1 (4%)	0	1 (12%)	
Initial Gleason score, n (%)				
3+3	8 (33%)	4 (25%)	4 (50%)	0.558
3+4	8 (33%)	6 (37%)	2 (25%)	
4+3	5 (21%)	3 (19%)	2 (25%)	
4+4	3 (13%)	3 (19%)	0	
Neoadjuvant hormones, n (%)				
Yes	10 (42%)	8 (50%)	2 (25%)	0.388
No	14 (58%)	8 (50%)	6 (75%)	

Note: There were no statistically significant differences in the clinical characteristics between the two patient groups.

(1) Age at the time of MRI.

(2) Follow-up PSA closest to the time of MRI.

(3) Initial clinical stage information was not available in one patient.

Table 2

Sensitivity and Specificity for the Detection of Locally Recurrent Prostate Cancer at Two Different Cutoff Points.

		Cutoff Point 1 (1-2; no tumor versus 3-5; tumor)		Cutoff Point 2 (1-3, no tumor versus 4-5; tumor	
		T2-weighted MRI	**Multi-parametric MRI**	**T2-weighted MRI**	**Multi-parametric MRI**
Patient Level	**Reader 1**				
	Sensitivity (%)	81	94	38	81
	Specificity (%)	25	75	88	100
	Reader 2				
	Sensitivity (%)	81	81	13	81
	Specificity (%)	25	75	88	75
Prostate-Side Level	**Reader 1**				
	Sensitivity (%)	77	82	32	68
	Specificity (%)	58	88	93	100
	Reader 2				
	Sensitivity (%)	73	64	14	64
	Specificity (%)	58	88	92	92

Table 3

Quantitative MRI Parameters at the Prostate-Side Level.

	Biopsy Positive (n=22)	Biopsy Negative (n=26)	p Value
ADC (10^{-3} mm^2/s), median (range)	1.44 (2.47 - 0.87)	1.68 (2.81 - 1.05)	0.012
K^{trans} (1/min), median (range)	1.07 (0.10 - 4.13)	0.34 (0.07 - 1.43)	0.010
k_{ep} (1/min), median (range)	2.06 (0.35 - 8.70)	1.00 (0.18 - 3.05)	0.008
v_e, median (range)	0.58 (0.16 - 1.00)	0.68 (0.29 - 1.00)	0.478
AUGC90 (mM.s), median (range)	19.49 (5.79 - 42.70)	14.94 (6.52 - 38.47)	0.294
AUGC180 (mM.s), median (range)	54.70 (13.81 - 116.5)	50.24 (18.50 - 97.81)	0.552